Received: 22 December 2024 | Accepted: 23 June 2025

DOI: 10.1111/jopr.14096

ORIGINAL ARTICLE

Assessing the influence of titanium dioxide nanotubes incorporation on thermal and thermomechanical characteristics of 3D-printed denture base resin

Zaid Basil Al-enbary BDS[1] | **Ihab Nabeel Safi BDS, MSc, PhD**[1] | **Julfikar Haider BSc Eng, MA, PhD**[2]

[1]Department of Prosthodontics, College of Dentistry, University of Baghdad, Baghdad, Iraq

[2]Department of Engineering, Manchester Metropolitan University, Manchester, UK

Correspondence
Julfikar Haider, Department of Engineering, Manchester Metropolitan University, Manchester, M12 5GN, UK.
Email: j.haider@mmu.ac.uk

Abstract

Purpose: This study aims to evaluate the effects of adding titanium dioxide (TiO_2) nanotubes (NTs) to three-dimensional (3D) printed denture base resin on the thermal and thermomechanical properties, which have high clinical relevance.

Materials and Methods: TiO_2 NTs with dimensions of 30–70 nm in diameter and 2–4 µm in length were added to the denture base resin at concentrations of 0.0 (control), 1.0, 2.0, 3.0, 4.0, and 5.0 wt.%. A total of 120 samples were printed with 60 samples for hot-disc device tests (thermal conductivity [$\varkappa$], thermal diffusivity [D] and volumetric heat capacity [ρC_p] tests) and 60 samples for thermomechanical analyzer (TMA) device tests (coefficient of thermal expansion [CTE, α], thermal strain [ε], and elastic modulus in response to temperature changes). The collected data were analyzed with ANOVA followed by Tukey's post hoc test ($\alpha = 0.05$).

Results: The results revealed that increasing the TiO_2 NT concentration improved all the thermal properties. However, in the thermomechanical tests, an improvement was observed only in the 1.0 wt.% and 2.0 wt.% TiO_2 NT composite groups, and a significant decline was observed in the remaining groups. Fourier Transform Infrared Spectroscopy (FTIR) results revealed no alteration in the chemical structure of the resin. However, the degree of conversion (DC) of the nanocomposites after polymerization was significantly affected. The samples tested via field emission scanning electron microscopy (FESEM) with energy dispersive x-ray spectroscopy (EDX) revealed an even distribution of the TiO_2 NTs in the 3D-printed samples.

Conclusions: The improvement in the thermal and thermomechanical properties of the denture material could enhance patient satisfaction by providing better perceptions of hot and cold foods, reducing marginal deterioration, and increasing durability during mastication.

KEYWORDS

3D printing, acrylic resin, coefficient of thermal expansion, degree of conversion, modulus of elasticity, thermal conductivity, thermomechanical properties, titanium dioxide nanotubes

Three-dimensional (3D) printing is a production method that creates products through a layer-by-layer building approach[1] and is an attractive option for the production of complete dentures.[2,3] According to certain reports, the major benefit of 3D printing over the standard production chain is the decrease in the number of visits needed before final denture delivery to patients.[4] The common 3D printing technologies used for denture fabrication are stereolithography (SLA),[5,6] digital light processing (DLP),[6,7] and more recently introduced liquid crystal display (LCD).[2,6] However, the properties of 3D-printed resins (e.g., physical, mechanical, and thermal) are still inferior to those of the standard heat-cured acrylic resins.[8,9] The incorporation of nanoparticles into the photopolymer matrix is considered to

---

be a technique for improving the properties of 3D-printed resins.[9,10]

Polymeric nanocomposites (PNCs) are composed of a polymer matrix and nanoscale filler.[11] The properties of the nanocomposite material are determined by the nature, morphology, size, and concentration of the nanomaterials (NMs), and their interaction with and dispersion throughout the matrix resin, which limit the movement of the polymer chain. Consequently, an increased modulus is observed in polymer nanocomposite materials,[11–15] and their thermal properties become more favorable than those of pure polymer materials.[14] Titanium dioxide (TiO_2) is one such NM commonly used as a filler and has high thermal and chemical stability, hydrophilicity, biocompatibility, low toxicity, superior strength and good refractive index.[1]

The oral environment experiences temperature fluctuations as a result of food and drink consumption, as well as occlusal stresses, which may cause deformation of dental prostheses over time.[3,16] Fitted dental prostheses might thermally expand or contract in response to heat fluctuations. A significant difference in thermal expansion characteristics between different dental prosthetic parts (denture bases, artificial teeth, etc.) might result in the development of interfacial stress, which has been linked to marginal deterioration as one of the etiological factors.[16] Another drawback of acrylic denture resin is its low thermal conductivity, which leads to a decreased perception of taste among denture wearers, as food temperature is known to impact taste perception. When cold or hot food or drinks are swallowed, the oral mucosa temperature fluctuates briefly from 37°C to 70°C before returning to its usual physiological value. This disruption can cause dissatisfaction in older patients whose palate mucosa is partly or entirely covered with the denture base. A denture foundation with high thermal conductivity can protect tissue health, improve taste, and minimize the sensation of the prosthesis as a foreign body. Thermally conductive ceramics (metal oxides) are better additives than bulk metal powders due to their comparable thermal conductivity and lower density, which does not add too much weight to the prosthesis.[17]

The majority of previous studies associated with 3D-printed denture base resins and associated nanocomposites have focused on determining mechanical and physical properties.[9,12,18] The effects of adding nanoparticles to resin on the thermal and thermomechanical properties have not been extensively explored to date. This novel route of investigation is pivotal for understanding the performance of dentures in clinical conditions where a temperature rise in the oral cavity is commonly experienced during the intake of hot foods and drinks. Previous studies have used TiO_2 nanoparticles to enhance only the mechanical, physical, and antibacterial characteristics of the resulting 3D denture base resin composite,[1,19] and only one study has evaluated the effects of TiO_2 nanotubes (NTs) on the mechanical properties of 3D-printed resin composites.[8] To the best of the authors' knowledge, no studies have assessed the impact of the addition of TiO_2 nanotube filler on the thermal and thermomechanical properties of 3D-printed resins, which have significant clinical relevance for developing innovative and high-performing dentures. To address this gap, the aim of this study was to evaluate the impact of the addition of TiO_2 NTs on the thermal and thermomechanical properties of 3D-printed denture base materials. The null hypothesis states that the thermal and thermomechanical properties do not change significantly after the addition of TiO_2 NTs to 3D-printed denture base resin.

MATERIALS AND METHODS

Study design

The denture base resin used for sample fabrication via 3D printing was DentaBase (Asiga, Australia, compliant with EN ISO 13485:2016 and ISO 13485:2016). The manufacturer's data sheet indicates that the resin comprises urethan di-methacrylate (7,7,9 or 7,9,9)-trimethyl-4,13-dioxo-3,14-dioxa-5,12-diazahexadecane 1,16-diyl bismethacrylate, diphenyl(2,4,6-trimethylbenzoyl) phosphine-oxide, and tetrahydrofurfuryl-methacrylate, compatible with a 385 nm 3D printer. TiO_2 NTs (diameter: 30–70 nm; length: 2–4 μm) sourced from Hongwu, China, were utilized at concentrations of 0.0, 1.0, 2.0, 3.0, 4.0, and 5.0 wt.% to fabricate nanocomposites via incorporation with the resin. The overall number of samples was 120, comprising 60 samples for thermomechanical analyzer (TMA) device tests and 60 samples for hot-disc device tests. Ten samples ($n = 10$) were allocated to each test group (control [0.0], 1.0, 2.0, 3.0, 4.0, and 5.0 wt.% TiO_2 NTs incorporated composite groups). The investigation included tests for thermal conductivity (κ), thermal diffusivity (D), and volumetric heat capacity (ρC_p) conducted using a hot disc, as well as tests for the coefficient of thermal expansion (CTE or α), thermal strain (ϵ) and elastic modulus (EM) as a function of temperature variation were performed with a TMA device.

The effective sample size was calculated using G power software (version 3.1.9.7) with a power of study at 85%, an alpha error of probability of 0.05, an effect size of $F = 0.3$ (medium effect size), and six groups and five-point measurements (30°C, 40°C, 50°C, 60°C and 70°C). The sample size for each testing device was estimated to be 36 samples ($n = 6$), but 10 samples were considered for each group for a more powerful interpretation of the results.

Sample design and material preparation

The samples were digitally generated via computer-aided design (CAD) software, specifically 3D Builder from Microsoft Corporation (Figure 1a, b). The hot disc samples were 20 mm (r) × 15 mm (t),[20] and the TMA samples were cylindrical in shape and 2.5 mm (r) × 20 mm (l).[21] The design for the 3D printing file in standard tesselation language (STL) format was submitted to the application (Asiga Composer) as depicted in Figure 1c.

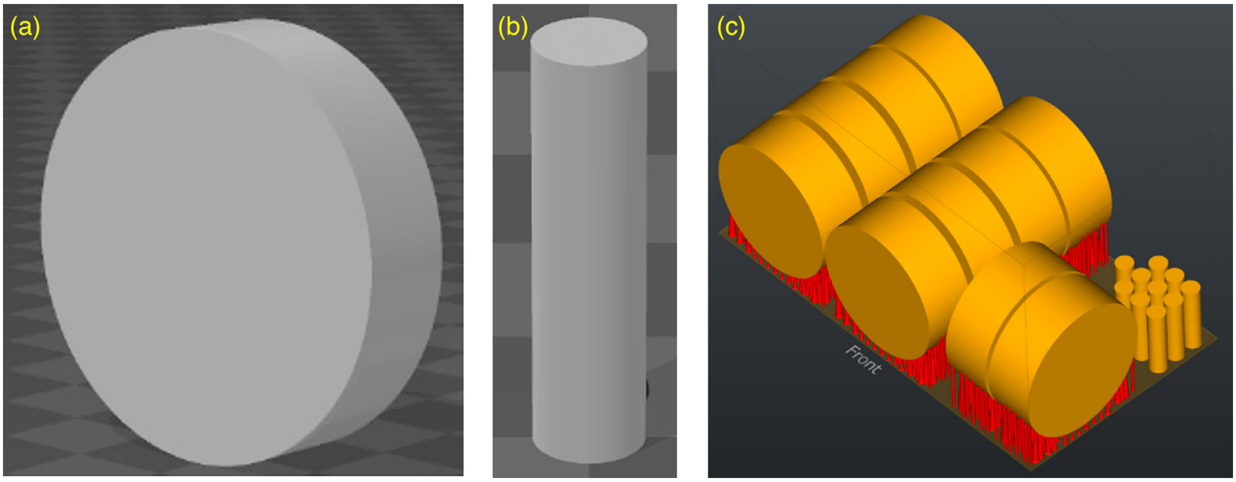

FIGURE 1 Digital design dimensions for (a) hot disc sample and (b) TMA sample; (c) Asiga Composer software showing the arrangement of the samples on the printing platform.

Titanium dioxide nanotube incorporation

Nanoparticles are maintained as powders that aggregate into clusters of individual particles due to superior inter-particle interactions caused by van der Waals forces.[22] Therefore, prior to blending them with 3D liquid resin, particles must be redispersed using ultrasonication with a dispersion medium without altering the properties of the original particles.[23] A specialized shaker (LC-3D Mixer Nextdent, South Korea) was initially used to ensure a uniform blend of printed denture base resin. A mixture of 99.9% ethyl alcohol (Honeywell, Germany) and titanium NTs (Hongwu, China) was subsequently prepared at a ratio of 3.0 mL of alcohol to 1.0 g of nanotube. This mixture was then subjected to ultrasonic treatment (MSE Soniprep 150, UK) for 3 min. The quantities of NTs added to the groups (control, 1.0, 2.0, 3.0, 4.0, and 5.0 wt.%) were 0.0 g, 2.5 g, 5 g, 7.5 g, 10 g, and 12.5 g, respectively. The resin for the denture base was combined with a suspension of TiO_2 NTs in a dark yellowish-brown glass container, which was sealed to prevent exposure to ambient light. The magnetic stirrer (alfa HS-860, Iran) facilitated the mixing of the denture base resin with TiO_2 NTs for 30 min at 60°C with the glass container partially opened to allow escape of evaporated alcohol, followed by sealing the glass container for an extended period of 8 h at room temperature (25°C± 5°C) to ensure uniform dispersion of the NTs.[8] For each group, 250 mL of resin was utilized, which was sufficient to print all the samples for that group. This determination was performed via Asiga software, which requires 200 mL plus an additional 50 mL to ensure adequate resin availability during the printing of the final layer.

Printing of 3D sample blocks

The samples were printed via a DLP 3D printer from Asiga, Australia. The following printing parameters were used: heater temperature of 30°C, light intensity of 19, offset of 0.09, XY scale of 1.007, slice thickness of 0.05 mm, separation velocity of 4.3 mm/s, separation pressure limit of 300 g/cm^2 [8], and wavelength of 385 nm (high power UV LED). The printing orientation of the samples was vertical (90^0 angle to the platform base),[24] and the printing time was 2 h and 4 min (10 disc-shaped and 10 cylindrical-shaped samples on the build platform). Upon filling the printer vat with the liquid polymer mixture, which consisted of resin combined with TiO_2 NTs, the lid was securely closed to prevent exposure of the mixture to ambient light. The DLP printer program divides the digital model of the samples into thin horizontal layers, measuring 50 µm for each layer. The DLP projector projected these layers onto the surface of the liquid resin, resulting in the solidification of the liquid polymer mixture, and upon draining out the liquid in the vat, the printed samples were exposed.

Cleaning, drying, and curing

The samples were carefully detached from the 3D printer platform utilizing a sharp blade and subjected to two cycles of ultrasonic cleaning (Clean I, Ackureta, Taiwan) for 3 min each. An additional 2 min was dedicated to cleaning the printed samples with 99.9% isopropyl alcohol[8] to eliminate any leftover uncured resin. Once the samples were thoroughly dried, they underwent polymerization following exposure to a light curing process inside a UV box (Ackureta, Taiwan) under the following conditions: UV wavelength = 385 nm LEDs, power = 65 watts, curing time = 30 min and curing temperature = 60°C according to the manufacturer's recommendations and Altarazi et al.[24] An acrylic bur and lathe polishing equipment were employed to finish and polish the sides of the samples that were connected to the platform and supports, and the samples were measured with a Vernier scale (Cachor, India).

Particle size analyzer, FESEM, EDX, and FTIR tests

The TiO_2 NT powder was measured using a particle size analyzer (PSA) (90Plus, Brookhaven, USA). A Field-Emission Scanning Electron Microscope (FESEM—INSPECT F50, FEI company, USA) was employed to examine the TiO_2 NT powder and fractured surface characteristics at different magnifications (500×, 15,000×, 20,000×, and 30,000×). Three sample groups (control, 1.0 % wt., and 5.0 wt.% TiO_2 NTs nanocomposites) along with TiO_2 NT powder were examined. Charges accumulate on the surface of the resin samples, which can cause visual distortions, blurring, or even damage because the samples are not conductive. To enhance image quality and disperse this charge, the samples were sputter-coated with gold to a coating thickness of approximately 1 nm. Energy dispersive X-ray (EDX) spectroscopy (MIRA3TESCAN, USA) was used for surface microanalysis. The chemical composition of the nanocomposite filler was revealed by combining this approach of surface chemical microanalysis with SEM. The results are shown in terms of both weight and atomic percentages.

Fourier Transform Infrared (FTIR) Spectroscopy (SHIMADZU/ Japan) was used to determine whether any chemical reactions occurred between the 3D-printed resin and the added TiO_2 NTs. FTIR spectra were obtained at wavelengths ranging from 4000 to 400/cm at 2/cm resolution. Five samples each from the control, 1.0, 2.0, and 5.0 wt.% TiO_2 NTs nanocomposite groups and TiO_2 NTs powder were tested, and the results of the nanocomposite groups were compared with those of the control group. Additionally, FTIR spectra were used to measure the degree of conversion (DC) during polymerisation based on Equation 1.[24–28] The liquid resin was scanned as the baseline, and compared to the printed nanocomposite samples after polymerization[25–28].

$$\mathrm{DC}\ (\%) = \left(1 - \frac{\left(\frac{\mathrm{T}_{1637}}{\mathrm{T}_{1608}}\right) \text{peak hights after polymerization}}{\left(\frac{\mathrm{T}_{1637}}{\mathrm{T}_{1608}}\right) \text{peak hights befor polymerization}}\right) \times 100 \qquad (1)$$

Thermal analysis procedure

Thermal conductivity ($\varkappa$), thermal diffusivity (D), and volumetric heat capacity (ρC_p) tests were conducted via the transient plane heat source (TPS) method (Hot disc TPS 500, Sweden). The probe (sensor) was placed between the plane surface of the two samples and functions as both a heat source and a temperature-sensing device.[29,30] The Kapton-type sensor has a disk form with a radius of 6.403 mm, a measurement time of 160 s, a heating power of 100 mW, and a sample temperature of 22°C. The analysis software for the TPS 500 instrument produced direct and spontaneous values for all three parameters.

A thermomechanical analyzer (TMA) (PTS 1000 LINSEIS, Germany) device was used for the CTE (α) and elastic moduli as a function of temperature change and thermal strain (ϵ) tests. The test sample was placed in the center of the sample holder; the tapered tip probe was placed over the center of the sample, 50 mN pressure was applied, and the rate of increase in temperature was 5 K/min.

Statistical analysis

Data analysis was conducted via Prism 8 (GraphPad Software, USA) and SPSS (Statistical Package for Social Science, version 21). The findings are presented through bar charts that represent the mean values and standard deviations as part of the descriptive analysis. One-way analysis of variance (ANOVA) was employed along with post hoc Tukey's HSD test. The Shapiro–Wilk test was used to determine the normality of the data distribution, and Levene's test was applied to check the homogeneity of the data. *p*-values exceeding 0.05, those below 0.05, and those below 0.01 denote non-significant, significant, and highly significant differences, respectively.

RESULTS

Microstructure and composition

It was determined that the NTs were 30–70 nm in diameter and 2–4 μm in length (Figure 2). However, the particle size analysis (PSA) of the TiO_2 NTs revealed that the effective particle size was 138 nm. As the NTs have elongated cylindrical shapes with one dimension at the microscale, the PSA results do not point to a precise tube dimension (length or diameter) but rather an average value of the particle size.

EDX mapping of the elemental composition of the 3D-printed resin without the incorporation of TiO_2 NTs included oxygen (O) and carbon (C); the 3D-printed resin after the incorporation of 1.0 wt.% TiO_2 NTs contained oxygen, carbon, and Ti as shown in Figure 3.

The layered structure of the printed samples from the side was visible, and the layer thickness matched the slice thickness set during printing (Figure 4a). The 1.0 wt.% nanocomposite group (Figure 4b) contained TiO_2 NTs with a high surface area as a result of the elongated cylindrical shape within the 3D-printed acrylic resin, and they were almost completely coated with the resin, indicating a high contact area between them. The increase in NT diameter measured could be due to the resin coating around the NTs. On the other hand, the 5.0 wt.% nanocomposite group (Figure 4c) showed some degree of aggregation of TiO_2 NTs as a result of an increasing filler load.

Figure 5a shows a comparison of the FTIR spectra of the 3D-printed resin, TiO_2 NTs, and 3D-printed resin mixed with

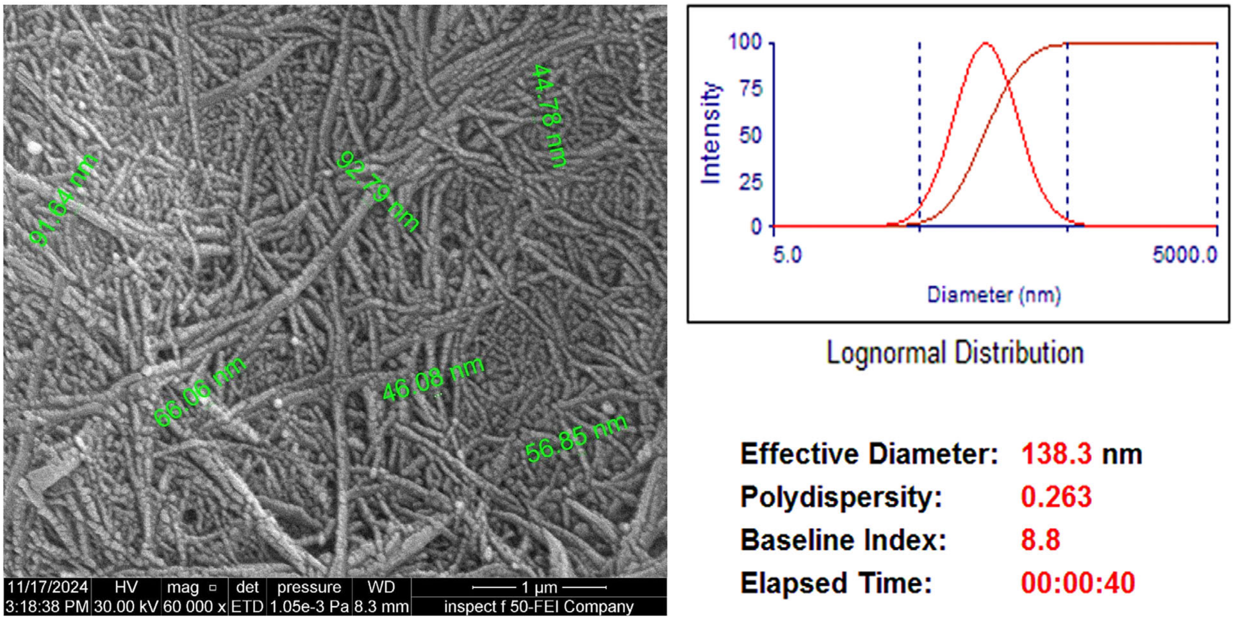

FIGURE 2 Microstructure analysis of TiO_2 nanotubes with particle size analysis results.

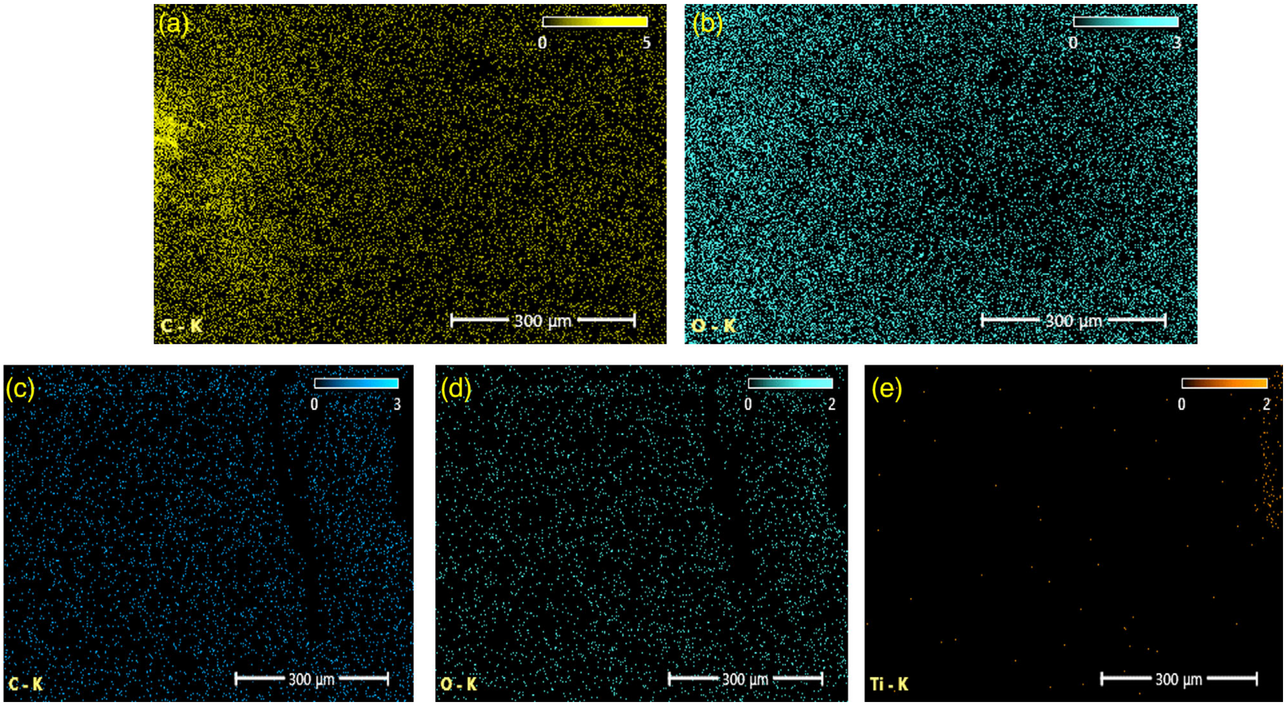

FIGURE 3 EDX mapping of only the 3D-printed denture base resin showing the distributions of (a) carbon and (b) oxygen, and after incorporation with 1.0 wt.% TiO_2 nanotubes showing distributions of (c) carbon, (d) oxygen, and (e) titanium.

TiO_2 NTs. No new bonds appeared when the 3D-printed resin and TiO_2 NTs were mixed, and all the bonds were the same in all the spectra except for those of the TiO_2 NTs. The DC values for the control, 1.0 wt.%, 2.0 wt.%, and 5.0 wt.% nanocomposites were 24.49%, 24.08%, 24.59% and 28.04%, respectively (Figure 5b).

Results from hot disc device tests

The thermal conductivity and thermal diffusivity results were directly proportional to the percentage of TiO_2 NTs, but the volumetric heat capacity results were indirectly proportional (Figure 6). Significant differences were found between the

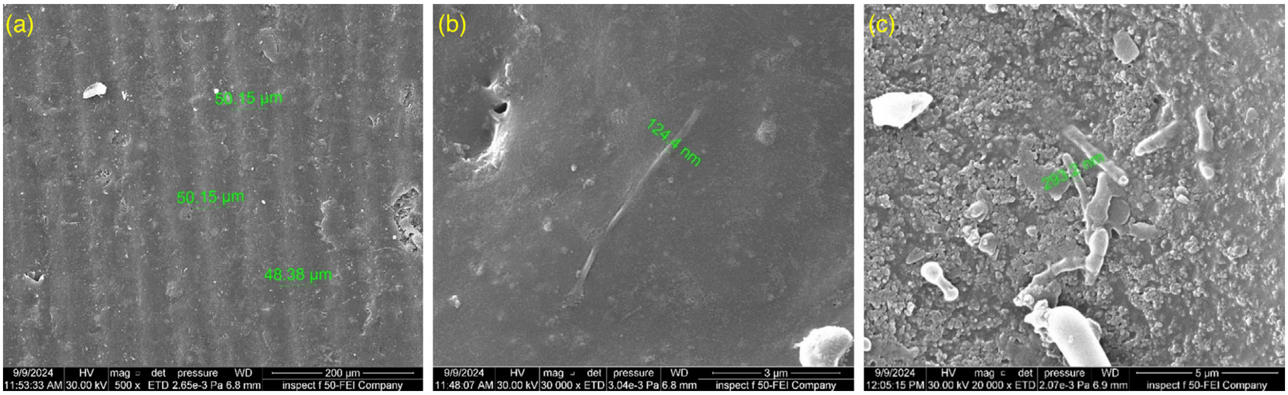

FIGURE 4 (a) FE-SEM images of pure 3D-printed acrylic (control group) showing a printing layer thickness of 50 µm, (b) Composite group showing high contact areas between 3D-printed TiO_2 nanotubes and PMMA resin, (c) Aggregation of 5 wt.%TiO_2 NTs within the acrylic resin.

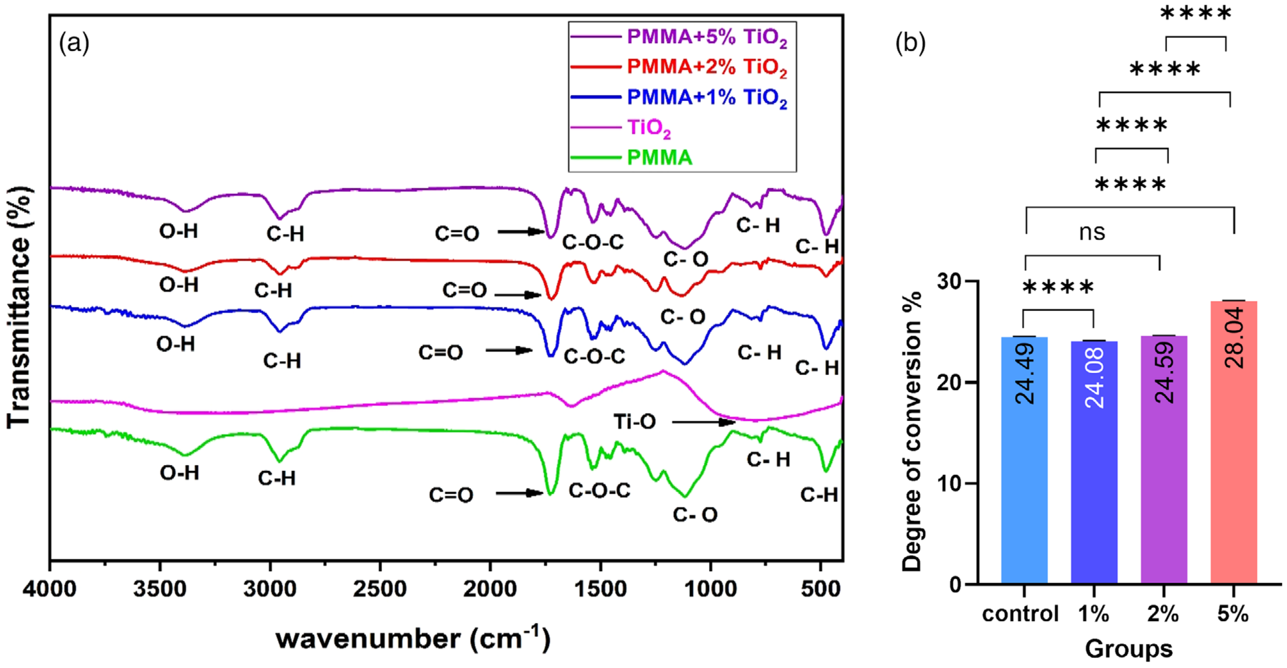

FIGURE 5 (a) Comparison of FTIR spectra for 3D-printed resin, TiO_2 NTs, and 3D-printed resin mixed with (1.0, 2.0, and 5.0 wt.%) TiO_2 NTs, and (b) degree of conversion results for the selected groups. ****indicates significant differences between the two groups, and ns denotes a nonsignificant difference.

control and other nanocomposite groups for all three thermal properties. In addition, significant differences were found among the nanocomposite groups, indicating that the addition of TiO_2 NTs between 1.0 and 5.0 wt.% influences the thermal properties.

Results from TMA device tests

The thermomechanical analysis (TMA) results are shown in Figure 7. As a function of temperature increase, the coefficients of thermal expansion (purple line) increased in a direct proportional relationship with increasing temperature. However, the elastic modulus (yellow line) increased as the temperature increased to 47.2°C, then the elastic modulus started to decrease with increasing temperature as it approached or exceeded the glass transition temperature of the 3D-printed resin.

The CTE results are presented in Figure 8a after comparing the control and nanocomposite groups at different temperatures. First, the α within the same group increased as the temperature increased. Second, when different groups at the same temperature were compared, α decreased as the TiO_2 NT filler content increased.

The thermal strain (ϵ) test results (Figure 8b) of the same group increased as the temperature increased. However, when different groups were compared at the same temperature, a greater addition of TiO_2 NTs caused a greater decrease in the strain percentage.

The elastic modulus results (Figure 8c) revealed that when different groups at the same temperature were compared, the elastic moduli increased with the addition of TiO_2 NTs, with

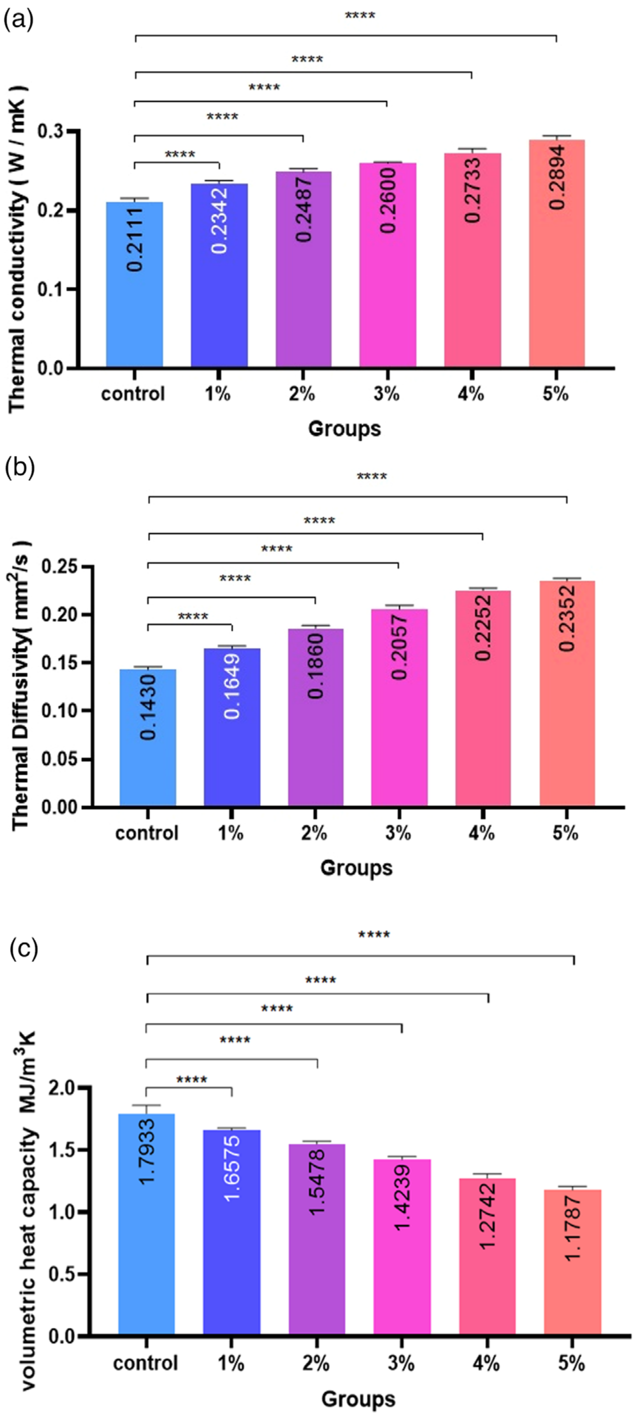

FIGURE 6 Results of the (a) thermal conductivity, (b) thermal diffusivity, and (c) volumetric heat capacity. **** indicates significant differences compared to the control group.

the highest value found in the 2.0 wt.% TiO_2 NT group followed by a gradual decrease in the remaining groups. However, when comparing the same group (control) of samples at different (increasing) temperatures, the elastic moduli increased as the temperature increased from 30°C to 50°C and then started to decrease as the temperature increased. It should be noted that significant differences were found among the nanocomposite groups for all the thermomechanical properties except the elastic modulus, which showed nonsignificant differences between the 4.0 and 5.0 wt.% groups at both 60° and 70°C.

DISCUSSION

The results showed that the thermal and thermomechanical properties of 3D-printed denture base resin changed significantly after the addition of TiO_2 NTs. An increase in the TiO_2 NTs concentration improved all the thermal properties. However, an improvement in the elastic modulus was observed only in the 1.0 wt.% and 2.0 wt.% TiO_2 NTs composite groups with a significant decline in the other groups. Therefore, the null hypothesis should be rejected, and the alternative hypothesis should be accepted.

Printing parameters and challenges

While printing the samples, the air trapped within the resin fluid could have led to the formation of voids in and between the printed layers, which influence the mechanical and thermal characteristics of the printed object.[8] Printing of the samples in this study was conducted with a layer thickness of 50 µm. As the thickness of the layer decreases, improved interlayer diffusion can reduce air voids.[31] Borella et al.[32] reported that printing samples with a layer thickness of 50 µm resulted in better properties than those of samples printed at 100 µm.

Multiple challenges such as print failure, particle sedimentation, and void entrapment were encountered during printing. First, multiple printing trials were carried out to choose which sample orientation was best for printing due to the large sample size as shown in Figure 9). Almost all printing errors were encountered with the larger hot disc samples. In this study, the samples were printed in a vertical orientation to achieve both successful printing and the best mechanical properties. Furthermore, other strategies such as increasing the first layer adhesion to the build plate by increasing the first layer thickness and increasing the amount of support were adopted to achieve successful printing of the samples. However, one issue associated with the vertical orientation was the longer printing time (2 h and 4 min) compared to a horizontal orientation (39 min) and possibly increased nanoparticle precipitation in the final layers of the samples, which could be directly proportional to the nanofiller load. Notably, the 45° printing time (2 h and 26 min) was slightly higher than that of the vertical orientation, possibly due to the higher volume of support material.

NM concentration and interaction with resin

In this work, one-dimensional (1D) NMs such as TiO_2 NTs were used as the filler. TiO_2 NTs are long,

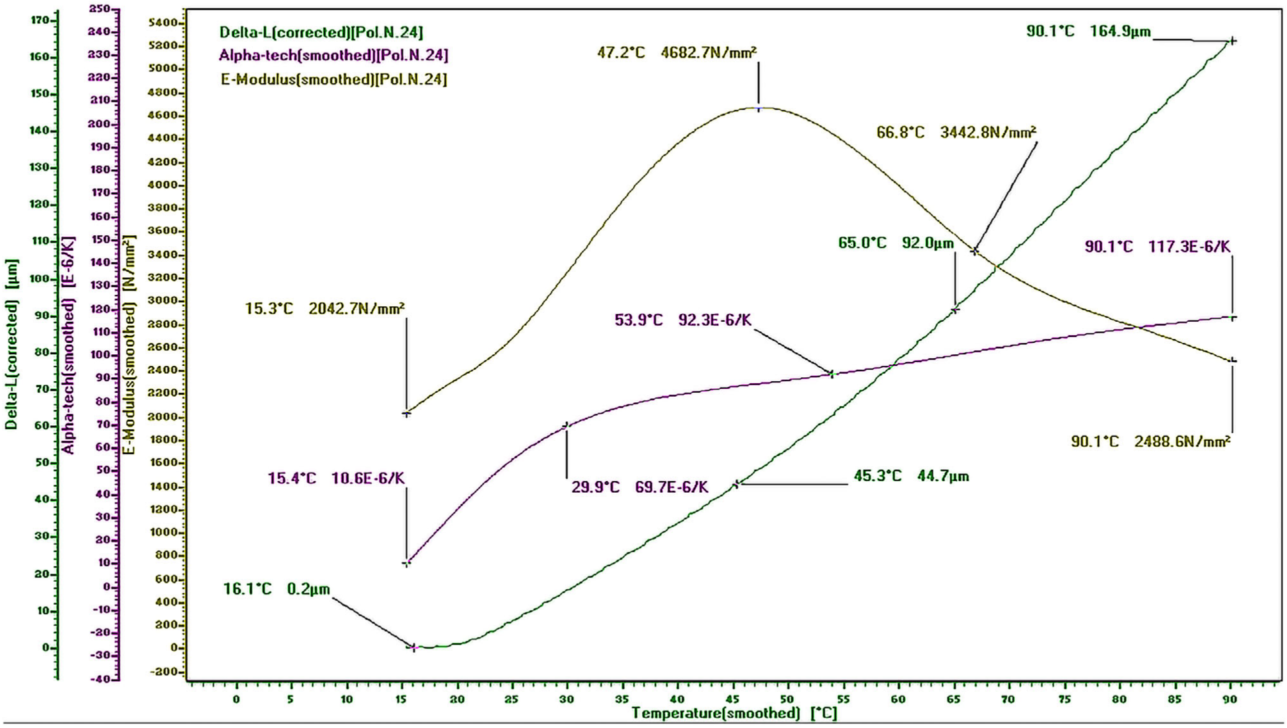

FIGURE 7 Thermomechanical analyzer (TMA, PTS 1000 LINSEIS, Germany) device test results.

cylinder-shaped with a hollow space similar to that in a tube. This enhances surface area-to-volume ratio (approximately 250 m^2/g), which is almost five times greater than that of TiO_2 nanoparticles, leading to increased nanotube-matrix interfacial bonding (interlocking) with a matrix with high interfacial shear strength.[33] These unique properties minimize polymerization shrinkage, enhance mechanical properties, and resist crack propagation.[8,33]

At TiO_2 NTs concentrations between 1.0 and 3.0 wt.%, most mechanical properties improve [8,34] while improvements in thermal properties occur at relatively higher concentrations (3.0–5.0 wt.% or higher).[14,34,35] As the aim was to improve the thermal properties without compromising the mechanical properties, five nanofiller concentrations (1.0, 2.0, 3.0, 4.0, and 5.0 wt.%) with an increase of 1.0 wt.% between each progressive group were selected for investigation. Furthermore, in this research, several printing trials were conducted to analyze the printability of various nanocomposite groups and to choose the best parameters and printing conditions. Adding TiO_2 NTs above 5.0 wt.% led to filler aggregation, preventing uniform distribution throughout the liquid resin, and a greater rate of NT precipitation, which affected printing quality and interfered with curing light penetration, resulting in a higher rate of printing failure. For example, minor printing errors (i.e., voids) started to appear at 3.0 wt.%, and the rate increased in the 4.0 wt.% group. Furthermore, printing failure occurred in a limited number of samples containing 4.0 wt.% NTs, but the failure rate increased in the 5.0 wt.% group, which could still be solved by changing the printing parameters. These final changes in parameters were used as the standard parameters during the printing of all groups in this research. However, above a 5.0 wt.% NT concentration, the printing failure could not be resolved even after adjusting the printing parameters.

Filler addition to 3D printing resin acts as contamination, and most 3D printing resins can accept the addition of 1.0 wt.% filler without any noticeable printing issues. As the filler concentration increases, more printing issues arise. First, the stability of the resin suspension during printing progressively compromised with increasing filler load due to an increasing rate of creaming or sedimentation resulting from differences in densities between the resin and NTs.[36] A higher rate of precipitation results, especially when printing larger disc-shaped samples in the vertical orientation. In addition, the loading of a high volume of NTs significantly alters the viscosity of the resin suspension, which prevents adequate recoating of the final printed layer with liquid resin during printing, ultimately leading to print failure.[36] However, this issue was addressed by heating the resin to 30°C. Second, the aggregation and sedimentation of the NTs results in an uneven distribution of fillers within the fabricated sample, hindering the entire geometry from achieving uniform properties[12,36] which was solved by both increasing the mixing time (8 h to ensure an even distribution of filler) and limiting the addition of TiO_2 NTs to a maximum of 5.0 wt.% percentage. Third, numerous composite vat photopolymerization strategies rely on liquid precursors that exhibit strong light permeability. Consequently, incorporating fillers in high percentages diminishes UV light penetration and curing depth, as scattering by the fillers can impact

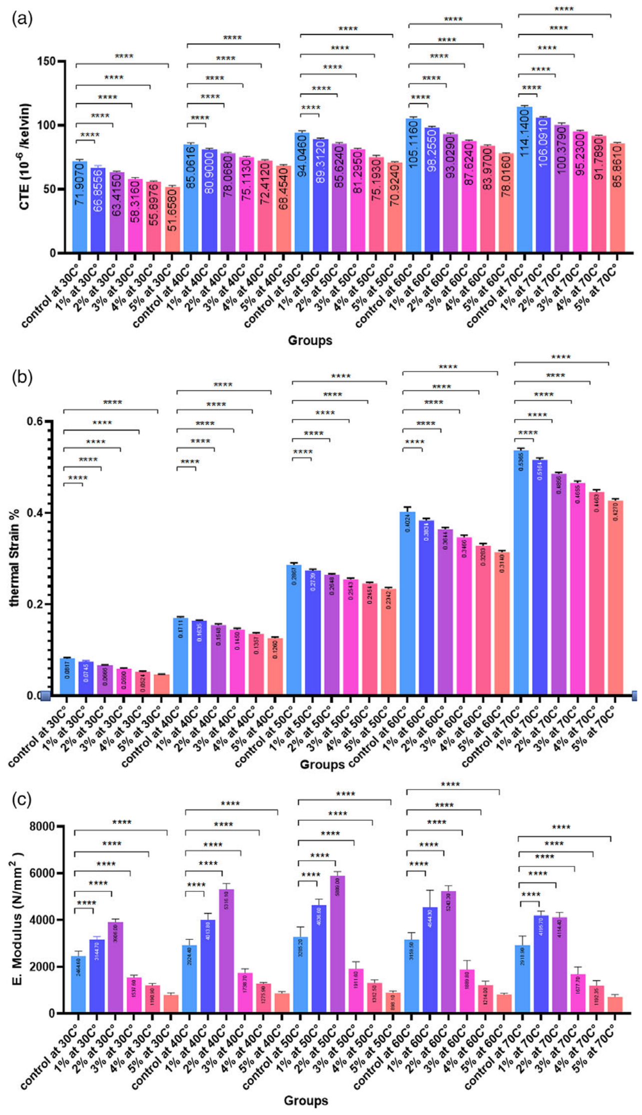

FIGURE 8 Test results for (a) Coefficient of thermal expansion, (b) Thermal strain, and (c) Elastic modulus. ****indicates significant differences compared to the control group.

interlayer curing.[36] Fourth, the formation of voids between subsequent layers of materials occurs as the NT concentration increases, leading to additional porosity during the printing process, which negatively impacts the mechanical and thermal performance.[31] However, this was addressed by printing in a thin layer (e.g., 50 μm).

FTIR and DC analysis

Figure 5a shows a comparison of the FTIR spectra of the 3D-printed resin, TiO_2 NTs, and 3D-printed resin mixed with 1.0, 2.0, and 5.0 wt.% TiO_2 NTs. No new bonds appeared when the 3D-printed resin and TiO_2 NTs were mixed, and all the bonds were the same in all the spectra except for those of the TiO_2 NTs. This clearly indicated that the mixing was purely physical rather than chemical.

Owing to the photocatalytic properties (photoinduced process) of TiO_2 NTs,[37] the addition of TiO_2 NTs accelerated photopolymerization. However, in this study, the addition of small percentages of TiO_2 NTs (1.0 wt.% and 2.0 wt.%) did not change the DC values (24.08% and 24.59%, respectively) compared to those of the control group (24.49%). The absence of a chemical reaction between the resin and TiO_2 NTs could support this observation. However, at 5.0 wt.%, the DC result (28.04%) increased by 3.55% compared to that of the control group. This improvement in DC with the addition of filler is consistent with the findings of Sulaiman et al.[38] In 3D-printed denture base resins, the complete conversion of aliphatic carbon-carbon double bonds is generally not achieved. The unconverted double bonds present in the resin result from two primary sources: unreacted monomers and pendant double bonds located at the ends of the polymer chains.[39] This can be explained by the fact that during polymerization, monomers experience a sequence of chemical events to produce polymer chains. Initially, monomers exist in a liquid form, allowing unrestricted movement and interaction with neighboring monomers. The elevated mobility facilitates the effective delivery of reactive species, enhancing polymerization and leading to a progressive increase in the DC until the gel point, at which point the polymer chains become interlinked where the mobility of the monomers diminishes markedly. The reduction in monomer mobility following the gel point hinders their diffusion and reaction with other monomers, which may affect the DC.[40] This reduction in monomer conversion increases in methacrylate resin at increased cross-linked levels.[41] In addition, the large sample size printed in this research (discs of 40 mm in diameter and 15 mm in thickness, and cylinders of 20 mm in length and 5 mm in diameter) would limit penetration of curing light. Also, long printing time results in sedimentation and affects the homogeneity of the final layers and composition, which in turn affects the DC. The above reasons explain the low DC of the control group (24.49%).

The clinical relevance of DC% could be associated with the thermal, mechanical, and biocompatibility properties of the 3D-printed denture base resin reinforced with TiO_2 NTs. For example, there is a direct correlation between DC% and thermal conductivity. Since the rate of energy transfer between linked monomers is more than 100 times faster than that between non-linked monomers,[42] any improvement in DC% leads to enhanced thermal conductivity, which can positively affect taste perception and improve marginal integrity. Additionally, an improvement in DC% enhances some of the mechanical properties of 3D-printed resin,[24] including elastic modulus.[43] However, the mechanical properties of 3D-printed resin composites (especially the elastic modulus) depend on factors related to both the resin matrix and filler content.[44] The decline in the elastic modulus in the 5.0 wt.% group despite the increase in DC could be attributed to the aggregation of the NT filler, which at higher concentrations acts as a plasticizer. Again, a higher DC% decreases the amount of residual monomer, leading to a reduction in adverse reactions in the oral tissues.

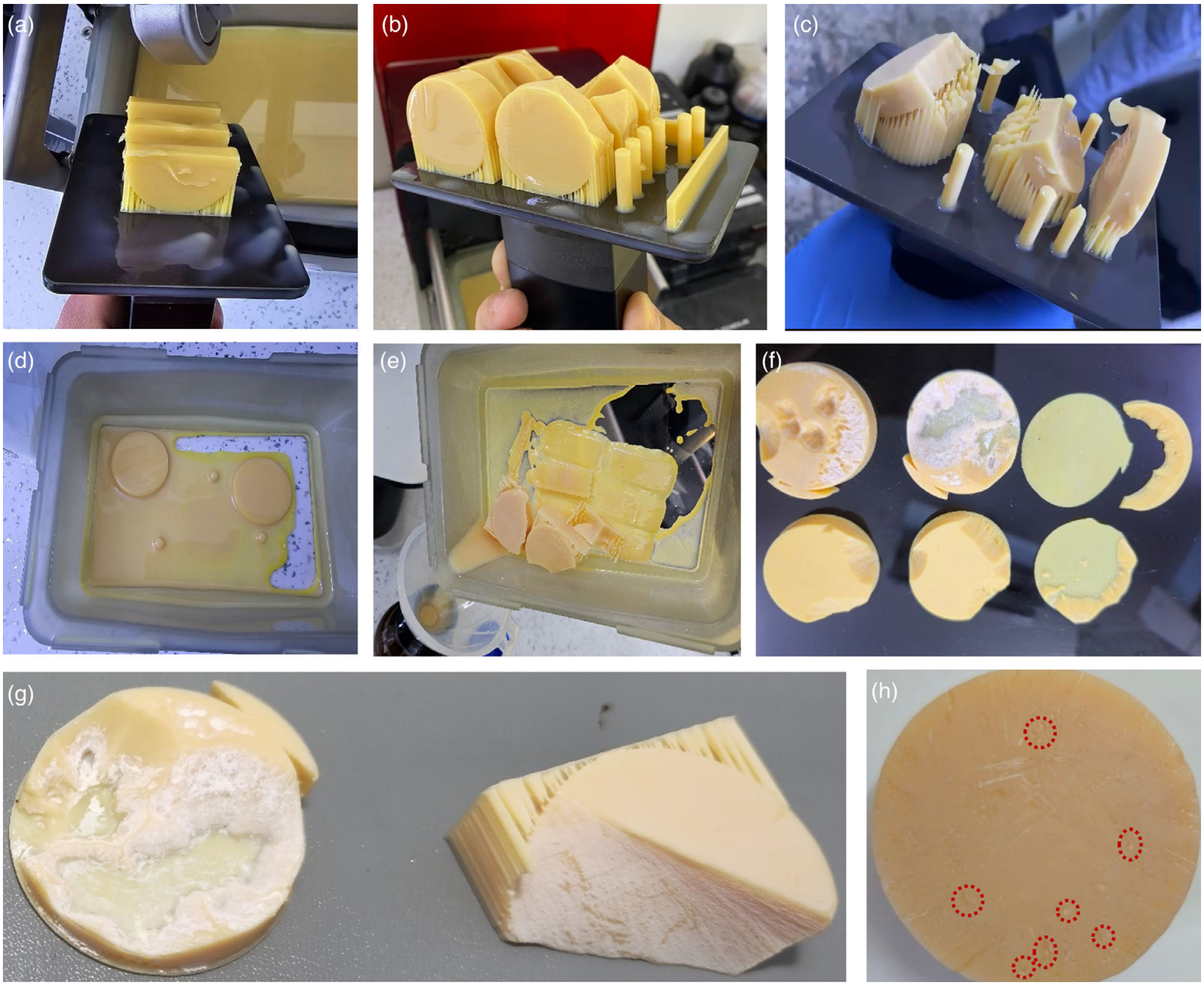

FIGURE 9 Different types of printing errors due to sample size: (a, b, c), Failure in printing the final layers of large samples with a high percentage of filler due to the excessive height of the samples, which is too long to print, leading to increased filler precipitation in the final layers. (d, e, f) Falling samples due to high suction and low adhesion between the samples and the plate. (g) Precipitations of the nanotube leading to printing failure due to high suction, (h) void entrapment within printed layers.

Analysis of thermal properties

The low thermal conductivity ($\varkappa$) values of the polymers can be attributed in part to the reduced crystallinity of their internal physical structure.[42,45] In this study, the 3D-printed resin consists of copolymers of different branched polymers (comprising urethan di-methacrylate and tetrahydrofurfuryl methacrylate), which reduce the thermal conductivity of the final printed resin sample. Additionally, experiments have indicated that $\varkappa$ is approximately 0.1–0.2 W/km for the van der Waals systems,[42,46,47]; hence, PMMA has a $\varkappa$ of approximately 0.20 W/km, with a peak value for amorphous polymers of approximately 0.4 W/km.[42,45,47,48] In this study, the mean value of $\varkappa$ of the 3D-printed resin (control group) was 0.2111 W/mK, which is in agreement with the findings of Xie et al.[48]

Additionally, research indicates that the thermal conductivity of a polymeric solid can be improved by incorporating a second component as a filler that possesses a relatively high thermal conductivity.[42] The filler composition (nanoparticles, NTs, chains/clusters)[45,49] and how it is arranged throughout the matrix[49] also influence the thermal conductivity. The thermal conductivity of TiO_2 NTs is approximately 0.40–0.84 W/mK (average 0.62 W/mK) at room temperature,[50] whereas that of PMMA is 0.20 W/km.[42,45,47,48] This work revealed that the $\varkappa$ increased with an increasing concentration of TiO_2 NTs added to the 3D-printed resin composite groups, with a maximum value for the 5% TiO_2 NT composite group. These findings agree with those of Mukherji,[42] Xu et al.,[45] and Hussain et al.[49]

Thermal diffusivity (D) is the rate of temperature transfer within a substance and is directly proportional to the thermal conductivity ($\varkappa$) and inversely proportional to the volumetric heat capacity (ρC_p). Rohde et al.[51] reported that the mean thermal diffusivity value of PMMA was approximately 0.114 ± 0.0035 mm^2/s at room temperature, while for the compact PMMA, the value was reported to be 0.15 mm^2/s.[52] Additionally, Sharma et al. reported that the thermal diffusivity of TiO_2 NPs was 0.425–0.430 mm^2/s at room temperature.[53] In this study, the mean thermal diffusivity value of the control group was 0.143 mm^2/s. Additionally, there was an increase in D, which was directly proportional to the percentage of TiO_2 NTs added to the 3D printing resin.

The volumetric heat capacity (ρC_p) is a fundamental physical property of matter and is characterized as the energy necessary to increase the temperature of a unit volume of a substance by one degree (°K or°C) under constant pressure. It shows an inverse relationship with the thermal conductivity and thermal diffusivity (D).[54,55] The mean value for the control group was 1.7933 MJ/m^{3}K, and the volumetric heat capacity decreased with increasing filler content, with a minimum mean value of 1.1787 MJ/m^{3}K for the 5% TiO_2 NT composite groups. These results agree with those of Fuchs et al.[54] and Sun et al.[55] in a way that the volumetric heat capacity is inversely proportional to the thermal conductivity and thermal diffusivity.

Analysis of thermomechanical properties

The CTE or α is defined as the ratio of the alteration in the length of the sample to the start length when the temperature changes, expressed as $\alpha = \Delta L / L^\circ \ \Delta T$.[56] An α mismatch among neighboring layers or components in systems may lead to structural deterioration, including interfacial delamination or cracking.[57] For the CTE test results, a comparison between groups at different temperatures reveals two important findings. First, when the same group is compared at different temperatures, the CTE increases as the temperature increases. This phenomenon occurs due to a rise in the kinetic energy of the atoms and molecules within the structure, leading to more vigorous vibrations and movements of its particles. Increasing the temperature leads to wider distances between atoms and molecular chains. Furthermore, as the temperature approaches or exceeds the glass transition temperature of the polymer, the CTE tends to rise sharply, leading to significant thermomechanical stresses within the structure.[58] Second, when different groups are compared at the same temperature, the CTE decreases as the TiO_2 NT filler content increases, which is consistent with the results of Safi.[14] This could be due to greater interfacial interactions between the nanofillers and the resin matrix, which limits chain mobility and macromolecules. The reduction in CTE would reduce marginal deterioration at the interface between different denture parts during the denture service life as a result of thermal fluctuations in the oral environment during the consumption of hot and cold drinks and food.

The thermal strain (ϵ) results from the anharmonic potential energy of a material. The anharmonicity leads to an increase in interatomic separation with increasing temperature, represented by $\epsilon = \alpha \times \Delta T$.[57,59] The control group has a mean thermal strain value of 0.0817% at 30°C, which increases as the temperature increases, with a mean value of 0.5365% at 70°C. A greater addition of TiO_2 NTs (5.0 wt.%) caused a greater decrease in the strain percentage, which was 0.046% at 30°C and 0.427% at 70°C. As the filler content increases, the chain mobility decreases,[14] leading to a lower strain.

The mean elastic modulus value for the control group was 2464.6 MPa at 30°C. The modulus with the addition of 2.0 wt.% TiO_2 NTs was the highest with a mean value of 3906.0 at 30°C, which was consistent with the results of Safi[14] and with those of AlGhamdi et al.[7] The values for all the nanocomposite groups exceeded 2000 MPa (recommended ISO 20795-1:2013) and were higher than those of the control group.[60] This enhancement could be attributed to two factors: first, the decreased elastic deformation of the organic matrix[61] because these nanofillers (which have large surface areas) fill the interstitial polymer regions (spaces between the polymer chains) and prevent the movement of the polymer chain segments.[62] Second, a network-like framework forms at high filler percentages.[61] Third, the Young's modulus of TiO_2 is estimated to be 118.54 GPa,[63] which is significantly greater than that of the pure polymer (2464.6 MPa). However, as the filler content increased above 2.0 wt.%, the elastic modulus decreased. The concentration-dependent shifts in the mechanical properties of a nanoparticle-filled polymer demonstrated that an increase in the proportion of NMs clearly resulted in the aggregation of the nanofiller.[64] At 1.0 and 2.0 wt.% TiO_2 NTs, the resin wets the nanoparticle surface, resulting in the immobilization of macromolecules on the filler surface, which subsequently leads to an increase in the mechanical properties.[65] In addition, above 2.0 wt.% TiO_2 NTs, the filler starts to aggregate, and the resin matrix fails to effectively wet the filler surface and behaves as a plasticizer.[49] This reduces the effective surface area for stress transfer and weakens the composite.[22] Additionally, the elastic moduli increase as the temperature increases from 30°C to 50°C and then start to decrease as the temperature increases to 70°C. This can be explained by the fact that as the temperature approaches or exceeds the glass transition temperature of a thermoset polymer, the mechanical properties of the polymer decline significantly,[58] resulting in a rubber-like nature, which is due to an increase in kinetic energy (quantifying motion capacity) among the atoms of the sample.

A comparison of previous reports[8,66] with the current results revealed that the addition of 2.0 wt.% TiO_2 NTs to 3D-printed resin could produce optimum mechanical, physical, thermal, and thermomechanical properties for the denture base.

Clinical significance, limitations, and future work

By incorporating TiO_2 NTs into 3D-printed denture base resins, several practical advantages can be achieved. First, there is an enhancement in thermal conductivity and thermal diffusivity, potentially leading to better perception of hot and cold foods and drinks and improved patient satisfaction. Second, during mastication and drinking of hot and cold food and drinks, different materials undergo different thermal expansion rates under a wide range of intraoral temperature changes, which could affect the marginal integrity and result in cracking or separation between the denture base and the artificial teeth. The addition of TiO_2 NTs resulted in a decrease in the thermal strain and CTE, which means that the interface among various denture parts would experience less marginal deterioration, leading to an improved shelf-life of the denture. Third, at elevated temperatures, the mechanical properties of the 3D-printed denture base resin decrease. Therefore, during the mastication of hot food, any reduction in thermomechanical properties might affect the integrity of the denture base. The improvement in the mechanical properties (elastic modulus) of the denture base due to the addition of TiO_2 NTs helps to better withstand the mastication force during the consumption of hot foods.

TiO_2 nanoparticles, a food additive commonly used in processed foods,[67] are biocompatible, noncytotoxic,[68] and have improved cell viability/proliferation at various concentrations.[69] TiO_2 NTs are used as coatings for titanium implant surfaces to accelerate osteoblast (bone cell) adhesion and proliferation at the biomaterial-tissue interface and enhance bone mineral formation.[70] However, it should be acknowledged that higher concentrations of TiO_2 in denture base materials can raise concerns about their biocompatibility. These include cytotoxic effects,[71] which may harm surrounding tissues, and trigger an inflammatory response in the oral tissues,[72] leading to discomfort or adverse reactions. Therefore, it is essential to balance the concentration of TiO_2 to maximize the thermomechanical properties while minimizing any risk of biocompatibility.

Additionally, it should be noted that printing was carried out using a single type of 3D-printed resin with a single layer thickness (50 µm), a single post-printing polymerization (30 min), one printing orientation (vertical), and the addition of a single nanofiller (TiO_2 NTs). The current results might differ from those of other resins, printing methods, and printing set-ups. Furthermore, it would be wise to perform tests with hybrid nanocomposites containing mixtures of different nanofillers with different natures, sizes, and geometries. Additionally, the tests conducted under dry conditions, without allowing them to age in various liquid media such as water, artificial saliva, or coffee, do not represent how they would operate in an actual oral environment. Consequently, further research will be carried out to evaluate the characteristics of the nanocomposite materials following accelerated aging under certain conditions.

CONCLUSIONS

Resin nanocomposites for denture bases were successfully printed by a DLP printer with TiO_2 NTs ranging between 1.0 wt.% and 5.0 wt.%. The EDX map and FE-SEM images revealed that the TiO_2 NTs were evenly dispersed throughout the 3D-printed resin. The FTIR results revealed that the addition of TiO_2 NTs to the resin could be considered only a physical blend with no alteration in chemical structure, though the addition of NTs could affect the DC of the nanocomposite groups studied. The thermal properties of the 3D-printed materials improved with increasing percentage of TiO_2 NTs. These properties include the thermal conductivity, thermal diffusivity, volumetric heat capacity, thermal strain, and CTE. The thermomechanical properties, such as the modulus of elasticity, improved in the 1.0 wt.% and 2.0 wt.% TiO_2 NTs composite groups but progressively decreased as the TiO_2 NTs percentage increased above 2.0 wt.%. The favorable thermal and thermomechanical properties obtained by adding an appropriate amount of TiO_2 NTs to the 3D-printed resin could lead to better outcomes for denture wearers in relation to structural integrity at higher mastication forces and perceptions of food taste.

ACKNOWLEDGMENTS

The authors would like to thank the University of Baghdad, Iraq, for providing all the technical support.

CONFLICT OF INTEREST STATEMENT

The authors declare no conflicts of interest.

DATA AVAILABILITY STATEMENT

The data that support the findings of this study are available from the corresponding author upon reasonable request.

ORCID

Zaid Basil Al-enbary BDS https://orcid.org/0009-0001-1008-6739
Ihab Nabeel Safi BDS, MSc, PhD https://orcid.org/0000-0002-1455-0439
Julfikar Haider BSc Eng, MA, PhD https://orcid.org/0000-0001-7010-8285

REFERENCES

1. Altarazi A, Haider J, Alhotan A, Silikas N, Devlin H. 3D printed denture base material: the effect of incorporating TiO(2) nanoparticles and artificial ageing on the physical and mechanical properties. Dent Mater. 2023;39(12):1122-36.
2. Wada J, Wada K, Garoushi S, Shinya A, Wakabayashi N, Iwamoto T, et al. Effect of 3D printing system and post-curing atmosphere on micro- and nano-wear of additive-manufactured occlusal splint materials. J Mech Behav Biomed Mater. 2023;142:105799.
3. Ellakany P, Fouda SM, Mahrous AA, Alghamdi MA, Aly NM. Influence of CAD/CAM milling and 3D-printing fabrication methods on the mechanical properties of 3-unit interim fixed dental prosthesis after thermo-mechanical aging process. Polymers. 2022;14(19):4103.
4. Unkovskiy A, Wahl E, Zander AT, Huettig F, Spintzyk S. Intraoral scanning to fabricate complete dentures with functional borders: a proof-of-concept case report. BMC Oral Health. 2019;19(1):46.
5. Mian SH, Abouel Nasr E, Moiduddin K, Saleh M, Alkhalefah H. An insight into the characteristics of 3D printed polymer materials for orthoses applications: experimental study. Polymers. 2024;16(3):403.
6. Schittecatte L, Geertsen V, Bonamy D, Nguyen T, Guenoun P. From resin formulation and process parameters to the final mechanical properties of 3D printed acrylate materials. MRS Commun. 2023;13(3):357-77.
7. AlGhamdi MA, Fouda SM, Taymour N, Akhtar S, Khan SQ, Ali MS, et al. Comparative evaluation of TiO(2) nanoparticle addition and postcuring time on the flexural properties and hardness of additively fabricated denture base resins. Nanomaterials. 2023;13(23):3061.

8. Mhaibes AH, Safi IN, Haider J. The influence of the addition of titanium oxide nanotubes on the properties of 3D printed denture base materials. J Esthet Restor Dent. 2024;36(11):1574-90.
9. Al-Sammraaie MF, Fatalla AA, Atarchi ZR. Assessment of the correlation between the tensile and diametrical compression strengths of 3D-printed denture base resin reinforced with ZrO2 nanoparticles. J Bagh Coll Dent. 2024;36(1):44-53.
10. Khalid RR, Fatalla AA, Matheel A, Johari Y, Beh YH, Abdullah JY. The impact of adding carbon nanotubes to 3D printed denture base resin on denture adaption, diametral compression, and tensile strength. J Int Dent Med Res. 2024;17(4):1517-26.
11. Gad M, Abualsaud R, Rahoma A, Al-Thobity AM, Alabidi K, Akhtar S. Effect of zirconium oxide nanoparticles addition on the optical and tensile properties of polymethyl methacrylate denture base material. Int J Nanomed. 2018;13:283-92.
12. Majeed HF, Hamad TI, Bairam LR. Enhancing 3D-printed denture base resins: a review of material innovations. Sci Prog. 2024;107(3):368504241263484.
13. Ali AA, Safi IN. Impact of nano-cellulose fiber addition on physico-mechanical properties of room temperature vulcanized maxillofacial silicone material. J Taibah Univ Med Sci. 2023;18(6):1616-26.
14. Safi IN. Evaluation the effect of nano-fillers (TiO2, AL2O3, SiO2) addition on glass transition temperature, E-Moudulus and coefficient of thermal expansion of acrylic denture base material. J Bagh Coll Dent. 2014;26(1):37-41.
15. Moudhaffar M, Ihab NS. Evaluation the effect of modified nano-fillers addition on some properties of heat cured acrylic denture base material. J Bagh Coll Dent. 2011;23(3):23-29.
16. Pinto-Sinai G, Brewster J, Roberts H. Linear coefficient of thermal expansion evaluation of glass ionomer and resin-modified glass ionomer restorative materials. Oper Dent. 2018;43(5):E266-EE72.
17. Yesildal F, Kul E, Yesildal R, Matori KA. Investigation of the thermal conductivity and flexural strength of polymethylmethacrylate denture base material with SiC and Al2O3 added. Mater Plast. 2021;58(2):91-99.
18. Yu H-J, Kang Y-J, Park Y, Kim H, Kim J-H. A comparison of the mechanical properties of 3D-printed, milled, and conventional denture base resin materials. Dent Mater J. 2024;43(6):813-21.
19. Bernasconi R, Bellè U, Brigatti S, Diamanti MV. 3D printing of photocatalytic nanocomposites containing titania nanoparticles. Addit. Manuf. 2024;79:103916.
20. ISO. ISO 22007-2:2022. Plastics-Determination of Thermal Conductivity and Thermal Diffusivity—Part 2: Transient plane heat source (hot disc) method. ISO; 2022.
21. ISO. ISO 11359-2:2021; Thermomechanical Analysis (TMA)—Part 2: Determination of Coefficient of Linear Thermal Expansion and Glass Transition Temperature. ISO; 2021.
22. Khdier HM, Husham KAF, Shali WM, Al-Atabi HA. Interfacial effects on mechanical, thermal and electrical properties of polymer-based nanocomposites: a review. Ann Chim Sci Mat. 2024;48:857-69.
23. Glaubitz C, Rothen-Rutishauser B, Lattuada M, Balog S, Petri-Fink A. Designing the ultrasonic treatment of nanoparticle-dispersions *via* machine learning. Nanoscale. 2022;14(35):12940-50.
24. Altarazi A, Haider J, Alhotan A, Silikas N, Devlin H. Assessing the physical and mechanical properties of 3D printed acrylic material for denture base application. Dent Mater. 2022;38(12):1841-54.
25. Ucuncu MK, Celiksoz O, Sen E, Yucel YY, Dinc B. Investigation of the degree of monomer conversion in dental composites through various methods: an in vitro study. Appl Sci. 2024;14(11):4406.
26. Dantagnan C-A, François P, Le Goff S, Attal J-P, Dursun E. Degree of conversion of 3D printing resins used for splints and orthodontic appliances under different postpolymerization conditions. Clin Oral Investig. 2023;27(6):2935-42.
27. Berghaus E, Klocke T, Maletz R, Petersen S. Degree of conversion and residual monomer elution of 3D-printed, milled and self-cured resin-based composite materials for temporary dental crowns and bridges. J Mater Sci Mater Med. 2023;34(5):23.
28. de Araujo LOF, Barreto O, de Mendonça AAM, França R. Assessment of the degree of conversion in light-curing orthodontic resins with various viscosities. Appl Adhes Sci. 2015;3:1-7.
29. Gustafsson SE, Mihiretie BM, Gustavsson MK. Measurement of thermal transport in solids with the hot disc method. Int J Thermophys. 2024;45(1):1–23.
30. Bauzin J-G, Laraqi N. New thermal analysis of the hot disc method based on explicit analytical developments. Int J Therm Sci. 2024;195:108645.
31. Benamira M, Benhassine N, Ayad A, Dekhane A. Investigation of printing parameters effects on mechanical and failure properties of 3D printed PLA. Eng Fail Anal. 2023;148:107218.
32. Borella PS, Alvares LAS, Ribeiro MTH, Moura GF, Soares CJ, Zancopé K, et al. Physical and mechanical properties of four 3D-printed resins at two different thick layers: an in vitro comparative study. Dent Mater. 2023;39(8):686-92.
33. Abdulrazzaq Naji S, Behroozibakhsh M, Jafarzadeh Kashi TS, Eslami H, Masaeli R, Mahgoli H, et al. Effects of incorporation of 2.5 and 5 wt% TiO(2) nanotubes on fracture toughness, flexural strength, and microhardness of denture base poly methyl methacrylate (PMMA). J Adv Prosthodont. 2018;10(2):113-21.
34. Mat Yazik MH, Sultan MTH, Jawaid M, Abu Talib AR, Mazlan N, Md Shah AU, et al. Effect of nanofiller content on dynamic mechanical and thermal properties of multi-walled carbon nanotube and montmorillonite nanoclay filler hybrid shape memory epoxy composites. Polymers. 2021;13(5):700.
35. Chen J, Gao X, Song W. Effect of various carbon nanofillers and different filler aspect ratios on the thermal conductivity of epoxy matrix nanocomposites. Results Phys. 2019;15:102771.
36. Shah DM, Morris J, Plaisted TA, Amirkhizi AV, Hansen CJ. Highly filled resins for DLP-based printing of low density, high modulus materials. Addit Manuf. 2021;37:101736.
37. Macwan DP, Dave PN, Chaturvedi S. A review on nano-TiO2 sol–gel type syntheses and its applications. J Mater Sci. 2011;46(11):3669-86.
38. Sulaiman MM, Fatalla AA, Haider J. The impact of incorporating grapefruit seed skin particles into 3D-printed acrylic resin on mechanical properties. prosthesis. 2024;6(6):1420-36.
39. Collares FM, Portella FF, Leitune VC, Samuel SM. Discrepancies in degree of conversion measurements by FTIR. Braz Oral Res. 2013;27(6):453-54.
40. Kirby S, Pesun I, Nowakowski A, França R. Effect of different post-curing methods on the degree of conversion of 3D-printed resin for models in dentistry. Polymers. 2024;16(4):549.
41. Moraes LGP, Rocha RSF, Menegazzo LM, Araújo EBD, Yukimito K, Moraes JCS. Infrared spectroscopy: a tool for determination of the degree of conversion in dental composites. J Appl Oral Sci. 2008;16(2):145-49.
42. Mukherji D. Thermal conductivity of polymers: a simple matter where complexity matters. Macromol Rapid Commun. 2024;45(24):2400517.
43. Petronijevic Sarcev B, Balos S, Markovic D, Sarcev I, Vukcevic M, Labus Zlatanovic D, et al. Effect of the degree of conversion on mechanical properties and monomer elution from self-, dual- and light-cured core composites. Materials. 2021;14(19):5642.
44. Ling L, Lai T, Malyala R. Mechanical properties and degree of conversion of a novel 3D-printing model resin. Polymers. 2024;16(24):3562.
45. Xu S, Liu J, Wang X. Thermal conductivity enhancement of polymers via structure tailoring. J Enhanc Heat Transf. 2020;27(5):463–89.
46. Ginzburg VV, Yang J. Modeling the Thermal Conductivity of Polymer-Inorganic Nanocomposites. In: Ginzburg VV, Hall LM, editors. Theory and modeling of polymer nanocomposites. Cham: Springer International Publishing; 2021. p. 235–57
47. Li B, DeAngelis F, Chen G, Henry A. The importance of localized modes spectral contribution to thermal conductivity in amorphous polymers. Commun Phys. 2022;5(1):323.
48. Xie X, Li D, Tsai T-H, Liu J, Braun PV, Cahill DG. Thermal conductivity, heat capacity, and elastic constants of water-soluble polymers and polymer blends. Macromolecules. 2016;49(3):972-78.

49. Hussain SA, Al-Sarraf AR. Study the contrast of thermal expansion behavior for PMMA denture base, single and hybrid reinforced using the thermomechanical analysis technique (TMA). AIP Conf Proc. 2023;2769:20027.
50. Gao T, Jelle B. Thermal conductivity of TiO2 nanotubes. J Phys Chem C. 2013;117:1401–8.
51. Rohde M, Hemberger F, Bauer T, Blumm J, Fend T, Häusler T, et al. Intercomparison of thermal diffusivity measurements on CuCrZr and PMMA. HTHP. 2014;42:1-6.
52. Milošev I, Hamulic D, Rodič P, Carrière C, Zanna S, Budasheva H, et al. Siloxane polyacrylic sol-gel coatings with alkly and perfluoroalkyl chains: synthesis, composition, thermal properties and log-term corrosion protection. Appl Surf Sci. 2021;574:151578.
53. Sharma G, Bansal A, Singh R. Thermal coefficients of Earth fuller reinforced with nano-oxide particles. Nano Express. 2021;2(1):10024.
54. Fuchs S, Förster HJ, Norden B, Balling N, Miele R, Heckenbach E, et al. The thermal diffusivity of sedimentary rocks: empirical validation of a physically based $\alpha - \varphi$ relation. J Geophys Res Solid Earth. 2021;126(3):e2020JB020595.
55. Sun S, Gu L, Yang Z, Lin H, Li Y. Thermophysical properties of natural gas hydrates: a review. Natural Gas Industry B. 2022;9(3):246-63.
56. Krzak A, Nowak AJ, Heljak M, Antonowicz J, Garg T, Sumption M. Mechanical and thermal analysis of duroplastic matrix composites over a range of temperatures. Polymers. 2024;16(5):606.
57. Kim J-H, Jang K-L, Ahn K, Yoon T, Lee T-I, Kim T-S. Thermal expansion behavior of thin films expanding freely on water surface. Sci Rep. 2019;9:7071.
58. Lahokallio S, Hoikkanen M, Vuorinen J, Frisk L. High-temperature storage testing of ACF attached sensor structures. Materials. 2015;8:8641-60.
59. Hofmann P. Solid state physics: an introduction. Wiley; 2015.
60. ISO. ISO 20795-1:2013; Dentistry—base polymers—Part 1: Denture base polymers. International Organization for Standardization (ISO), 2021.
61. Aminoroaya A, Neisiany RE, Khorasani SN, Panahi P, Das O, Madry H, et al. A review of dental composites: challenges, chemistry aspects, filler influences, and future insights. Compos. B Eng. 2021;216:108852.
62. Fatalla AA, Tukmachi MS, Jani GH. Assessment of some mechanical properties of PMMA/silica/zirconia nanocomposite as a denture base material. IOP Conf Ser Mater Sci Eng. 2020;987(1):012031.
63. Liu X, Fu J. Electronic and elastic properties of the tetragonal anatase TiO2 structure from first principle calculation. Optik. 2020;206:164342.
64. Khan RAA, Zulfqar A, Mateen M, Hussain M, Rasool RT, Ashraf GA, et al. Improvement of the glass transition temperature in novel molybdenum carbide doped polyaniline nanocomposites. Ceram Int. 2023;49(16):26322-30.
65. Serenko OA, Roldughin VI, Askadskii AA, Serkova ES, Strashnov PV, Shifrina ZB. The effect of size and concentration of nanoparticles on the glass transition temperature of polymer nanocomposites. RSC Adv. 2017;7(79):50113-20.
66. Anti DWK, Mukaromah AH, Subri M, Pujianto ME. An overview of titanium dioxide effect on mechanical properties of PMMA-TiO2 nanocomposites. J Int Dent Med Res. 2023;16(4):1797-803.
67. Dudefoi W, Villares A, Peyron S, Moreau C, Ropers M-H, Gontard N, et al. Nanoscience and nanotechnologies for biobased materials, packaging and food applications: new opportunities and concerns. Innovative Food Sci Emerg Technol. 2018;46:107-21.
68. Altarazi A, Jadaan L, McBain AJ, Haider J, Kushnerev E, Yates JM, et al. 3D-printed nanocomposite denture base resin: the effect of incorporating TiO_2nanoparticles on the growth of *Candida albicans*. J Prosthodont. 2024;33(S1):25-34.
69. Chellappa M, Anjaneyulu U, Manivasagam G, Vijayalakshmi U. Preparation and evaluation of the cytotoxic nature of TiO2 nanoparticles by direct contact method. Int J Nanomed. 2015;10(Suppl 1):31-41.
70. Neupane MP, Park IS, Bae TS, Yi HK, Watari F, Lee MH. Biocompatibility of TiO2 nanotubes fabricated on Ti using different surfactant additives in electrolyte. Mater Chem Phys. 2012;134(1):536-41.
71. Yadfout A, Asri Y, Merzouk N, Regragui A. Denture base resin coated with titanium dioxide (TiO2): a systematic review. Int J Nanomed. 2023;18:6941-53.
72. Asim FA, Al-Mosaweb EHA, Hussain WA. Studying the physical and biological characteristics of denture base resin PMMA reinforced with ZrO2 and TiO2 nanoparticles. KIJOMS. 2022;8(3):503-13.

How to cite this article: Al-enbary ZB, Safi IN, Haider J. Assessing the influence of titanium dioxide nanotubes incorporation on thermal and thermomechanical characteristics of 3D-printed denture base resin. J Prosthodont. 2025;1–14. https://doi.org/10.1111/jopr.14096